Discovery of novel spirocyclic inhibitors of fatty acid amide hydrolase (FAAH). Part 2. Discovery of 7-azaspiro[3.5]nonane urea PF-04862853, an orally efficacious inhibitor of fatty acid amide hydrolase (FAAH) for pain

Marvin J. Meyers *, Scott A. Long, Matthew J. Pelc, Jane L. Wang, Scott J. Bowen, Barbara A. Schweitzer, Mark V. Wilcox, Joseph McDonald, Sarah E. Smith, Susan Foltin, Jeanne Rumsey, Young-Sun Yang, Mark C. Walker, Satwik Kamtekar, David Beidler, Atli Thorarensen *

Pfizer Global Research & Development, St. Louis Laboratories, 700 Chesterfield Parkway West, Chesterfield, MO 63017, United States

ARTICLE INFO

ABSTRACT

Fatty acid amide hydrolase (FAAH) is an integral membrane serine hydrolase responsible for the degradation of fatty acid amide signaling molecules such as endocannabinoid anandamide (AEA), which has been shown to possess cannabinoid-like analgesic properties. Herein we report the optimization of spirocyclic 7-azaspiro[3.5]nonane and 1-oxa-8-azaspiro[4.5]decane urea covalent inhibitors of FAAH. Using an iterative design and optimization strategy, lead compounds were identified with a remarkable reduction in molecular weight and favorable CNS drug like properties. 3,4-Dimethylisoxazole and 1-methyltetrazole were identified as superior urea moieties for this inhibitor class. A dual purpose in vivo efficacy and pharmacokinetic screen was designed to be the key decision enabling experiment affording the ability to move quickly from compound synthesis to selection of preclinical candidates. On the basis of the remarkable potency, selectivity, pharmacokinetic properties and in vivo efficacy, PF-04862853 (**15p**) was advanced as a clinical candidate.

© 2011 Elsevier Ltd. All rights reserved.

Fatty acid amide hydrolase (FAAH) is an integral membrane serine hydrolase responsible for the degradation of fatty acid amide signaling molecules including the endocannabinoid anandamide (AEA).[1] It has been shown that inhibition of FAAH leads to elevated levels of AEA and analgesic effects in rodent models of pain without evidence of side effects commonly seen with cannabinoid receptor agonists, suggesting that inhibition of FAAH may result in a new class of analgesic agents.[2] In our previous report, we described our campaign to replace the methylenepiperidine core of our lead inhibitor of fatty acid amide hydrolase (FAAH), the clinical candidate PF-04457845 (**1**).[3] Compound **1** is a covalent inhibitor with exquisite potency and selectivity for FAAH, is orally efficacious at 0.1 mpk in a rat model of pain and is being evaluated in human clinical trials.[4]

In the previous report,[3] we described the successful identification of two new series of FAAH inhibitors with novel cores, 7-azaspiro[3.5]nonane and 1-oxa-8-azaspiro[4.5]decane, represented by lead compounds **2a–b** and **4**, respectively. These compounds have modest potency for FAAH (k_{inact}/K_i = 1570–3040 M^{-1} s^{-1}) but were found to lack efficacy at modest doses in the rat CFA model for pain (10 mpk, ip). Our medicinal chemistry optimization program aimed to reduce MW while improving FAAH k_{inact}/K_i potency to values greater than 2500 M^{-1} s^{-1}, minimizing in vivo clearance (CL <15), and improving oral in vivo efficacy to 1 mpk or less in rodent models of pain. Herein, we report our successful identification of a series of preclinical candidates, including clinical candidate PF-04862853 (**15p**).

Having identified two optimal spirocyclic cores, we outlined a parallel medicinal chemistry optimization strategy relying heavily on design of small, iterative compound libraries (~50 analogs/library) to optimize both the lipophilic tail group and the heteroaromatic head group (Chart 1). The aim of the compound libraries was to increase compound potency for FAAH while maintaining enzyme selectivity and CNS drug-like properties (e.g., MW <450, HBD <2, PSA <90 Å^3, $c \log P$ 2–5).[5] This strategy would enable the rapid identification of high quality compounds likely to have the physiochemical properties needed to advance into rodent efficacy models and into the clinic.
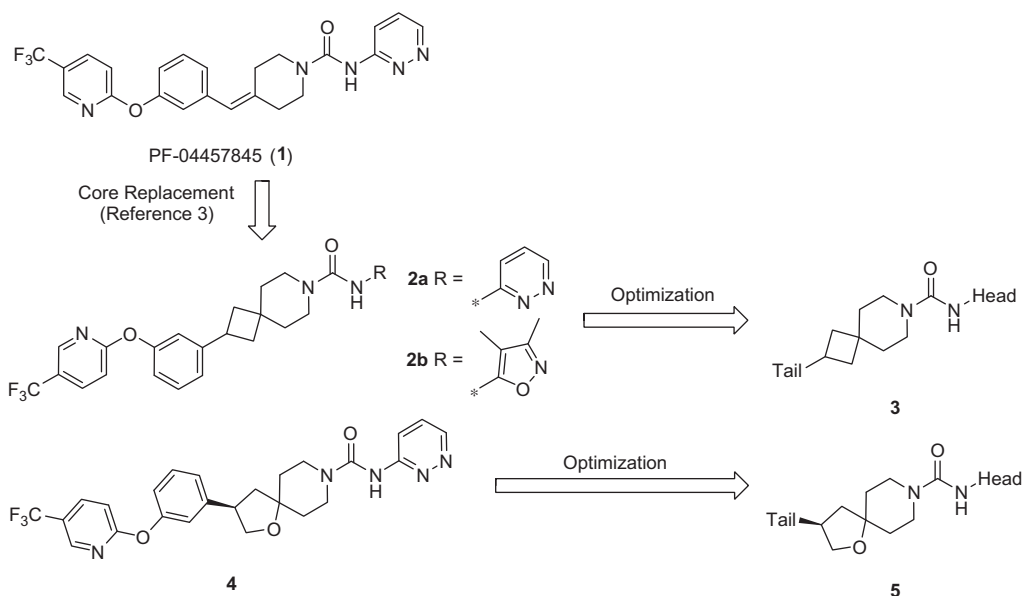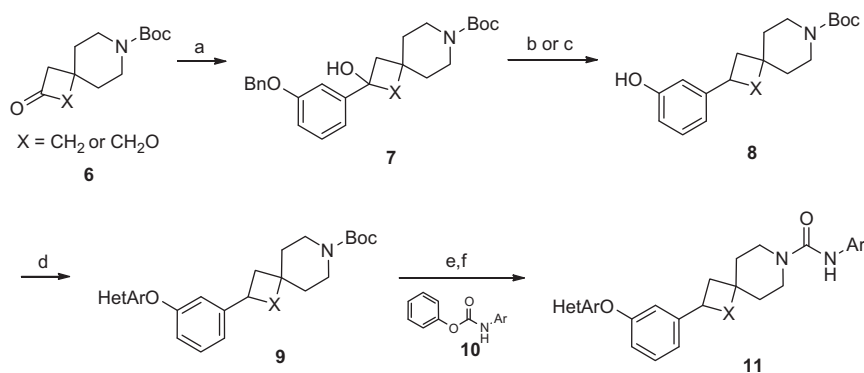

**Chart 1.** Medicinal chemistry optimization strategy.

Scheme 1. Library synthesis of terminal heteroaryl tail analogs. Reagents and conditions:[6] (a) 3-benzyloxyphenylmagnesium bromide, 2-MeTHF, 0 °C; (b) Raney Ni, EtOH, reflux; (c) (i) Et$_3$SiH, TFA, BF$_3$OEt$_2$, DCM, 0 °C; (ii) Boc$_2$O, TEA, DCM; (iii) H$_2$, 10% Pd/C, MeOH, 45 psi (36–38% from **6**); (d) heteroaryl chloride, cesium carbonate, DMF, 90 °C; (e) 4 N HCl/dioxane, DCM; (f) **10**, DIEA, CH$_3$CN, room temp.

Initially, the tail group was optimized while keeping the urea head group fixed as either 3-pyridazinyl or 3,4-dimethylisoxazol-5-yl. Libraries designed to replace the terminal heteroaryl group were prepared from the advanced intermediate phenol **8** as shown in Scheme 1.[6] Ketone intermediate **6** was treated with 3-benzyl-oxyphenylmagnesium bromide to give protected alcohol **7**. The alcohol was reduced during benzyl deprotection with Raney Ni to give phenol **8**. Alternatively, alcohol **7** was reduced with triethylsilane under strong acidic conditions. This method required repro-tection of the amine with Boc anhydride and removal of the

benzyl group. Phenol **8** was then treated with an array of hetero-aryl chlorides in the presence of cesium carbonate to give the crude displacement products. After concentration, treatment with HCl gave the Boc deprotected products which were concentrated, trea-ted with phenyl aryl carbamates **10**, and purified by reverse phase HPLC to give the final biaryl ether products **11**.

In an aim to reduce molecular weight to produce more CNS drug-like compounds,[5] the biaryl ether group was replaced with smaller substituted phenyl moieties using a modified Suzuki cou-pling strategy (Scheme 2).[6] Ketone **6** was reduced with sodium
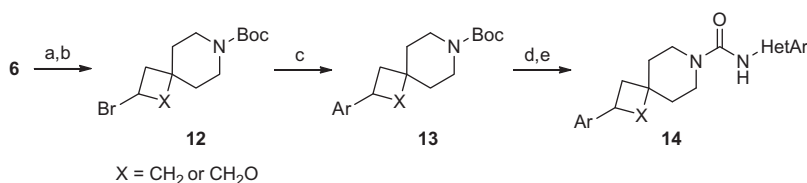
Scheme 2. Library synthesis of terminal truncated aryl tail analogs. Reagents and conditions:[6] (a) NaBH$_4$, MeOH, 0 °C (86%); (b) PPh$_3$, CBr$_4$, THF (42–51%); (c) ArB(OH)$_2$, NiI$_2$, LiHMDS, *trans*-1,2-aminohexanol, isopropanol; (d) 4 N HCl/dioxane, DCM; (e) **10**, DIEA, CH$_3$CN, room temp.
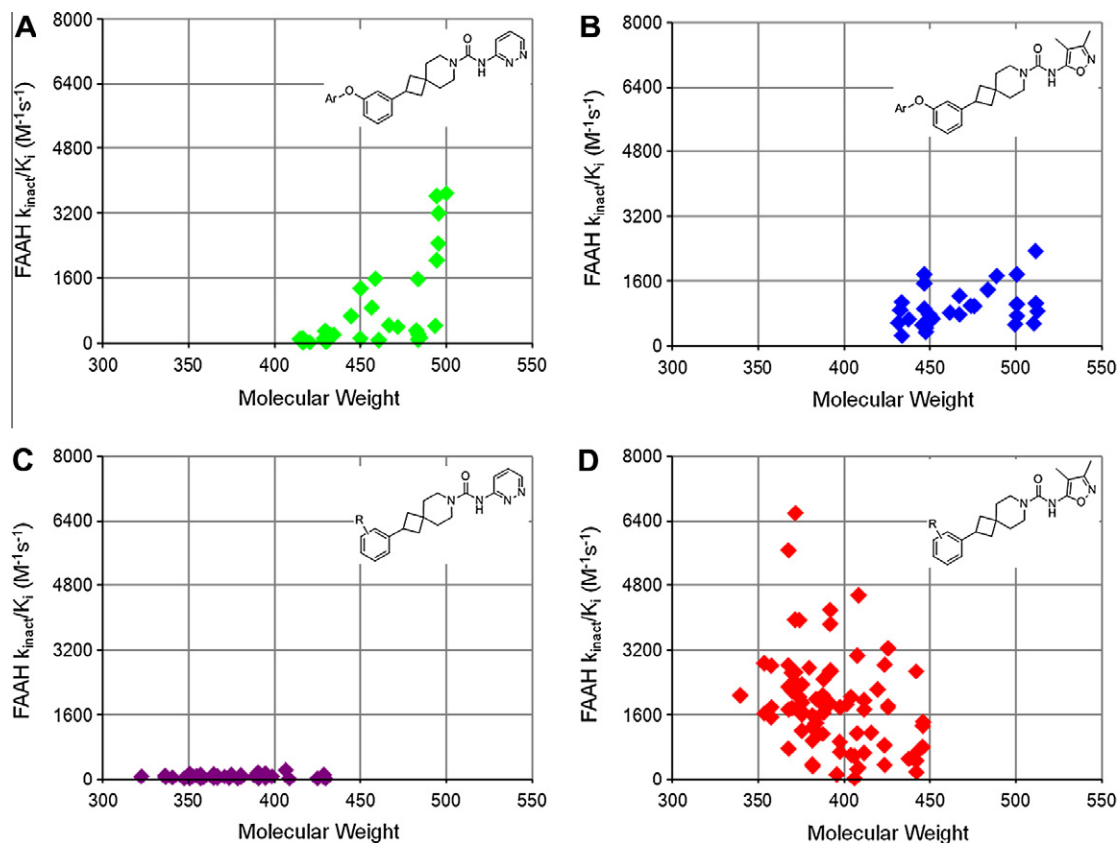
Figure 1. 7-Azaspiro[3.5]nonane tail group SAR for different tail/head group combinations. (A) Biaryl ether/pyridazine. (B) Biaryl ether/dimethylisoxazole. (C) Truncated phenyl/pyridazine. (D) Truncated phenyl/dimethylisoxazole.
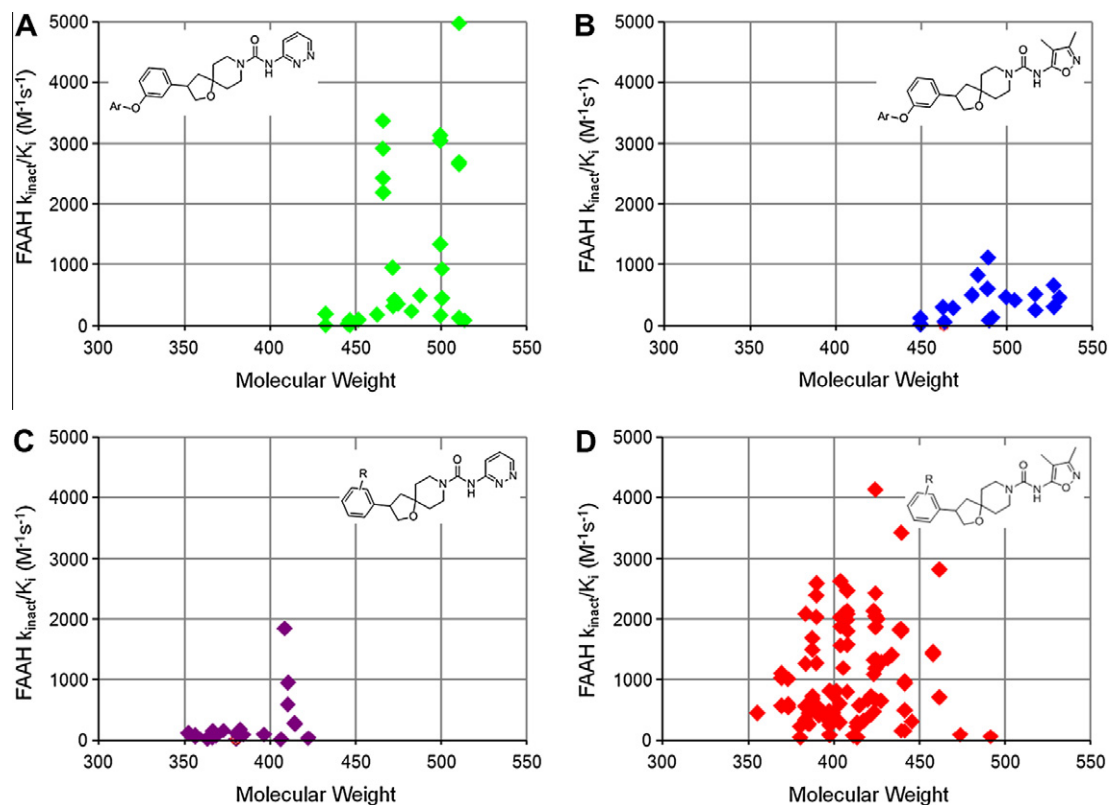
Figure 2. 1-Oxa-8-azaspiro[4.5]decane tail group SAR for different tail/head group combinations. (A) Biaryl ether/pyridazine. (B) Biaryl ether/dimethylisoxazole. (C) Truncated phenyl/pyridazine. (D) Truncated phenyl/dimethylisoxazole.

borohydride to give the alcohol which was readily converted to bromide **12** by treatment with triphenylphosphine and carbon tetrabromide. Bromide **12** was the key intermediate used to prepare libraries of truncated aryl tail groups using aryl boronic acids and the Ni-catalyzed Suzuki coupling methodology developed by Fu and co-workers.[7] Intermediate crude coupling products **13** were treated with HCl to remove the Boc protecting group, concentrated, exposed to heteroaryl phenyl carbamates **10** under mild basic conditions, and purified by reverse phase HPLC to give the final products **14**.

Analysis of hFAAH activity as a function of the tail group substitution revealed some interesting trends. Representative compounds from the 7-azaspiro[3.5]nonane series illustrate these trends as shown in Figure 1. Replacement of the terminal trifluoromethyl pyridyl group with other heterocycles resulted in only marginal gains in hFAAH potency with the 3-pyridazinyl head group being preferred over the 3,4-dimethylisoxazol-5-yl head group (Fig. 1A and B). Surprisingly, this trend was only observed for the biaryl ether tail group. Remarkably, truncation of the biaryl ether to a phenyl ring with small lipophilic substituents such as Cl, F, Me, OMe, CF$_3$, or OCF$_3$ gave compounds with a reduced molecular weight near 400 and significantly improved hFAAH activity (Fig. 1D; Table 1). This effect was observed only when combined with the 3,4-dimethylisoxazol-5-yl head group whereas the direct comparators in this class with the 3-pyridazinyl head group were only weakly active (Fig. 1C). As a result, subsequent libraries were designed focusing on optimization of the truncated aryl tail group with small lipophilic groups and the 3,4-dimethylisoxazol-5-yl head group (Fig. 1D).

Similar trends were observed for the 1-oxa-8-azaspiro[4.5]decane series (Fig. 2A–D). For this series, however, higher levels of FAAH potency were more readily achieved with the biaryl ethers/pyridazine tail/head group combination than with the truncated/dimethylisoxazole tail/head group combination. Like the 7-azaspiro[3.5]nonane series, subsequent libraries focused on optimization of the truncated aryl tail group with small lipophilic groups and the 3,4-dimethylisoxazol-5-yl head group (Fig. 2D). Other tail group derivatives were also explored but are outside the scope of this manuscript and will be reported elsewhere.

Specific representative examples truncated aryl tail analogs from the 7-azaspiro[3.5]nonane series (**15a–p**) and the 1-oxa-8-azaspiro[4.5]decane series (**16a–j**) are shown in Table 1. For the 7-azaspiro[3.5]nonane series, the simple phenyl analog (**15a**) was potent for human FAAH (hFAAH), but did not have sufficient potency against the rat FAAH (rFAAH) necessary for advancement into efficacy studies. Similarly, methoxyphenyl analogs (**15b–d**) were equipotent for hFAAH but insufficient for rFAAH. Interestingly, the corresponding trifluoromethoxyphenyl analogs (**15e–g**) had equipotency for hFAAH and rFAAH but greater sensitivity to the substitution pattern (i.e., 3-OCF$_3$ **15f** retained hFAAH and rFAAH potency but 2-OCF$_3$ **15e** and 4-OCF$_3$ **15g** were four to eightfold less potent). A similar hFAAH: rFAAH potency trend was observed for trifluoromethyl (**15h–j**) versus non-halogenated methyl (**15k**), and ethyl (**15l**) analogs. 3-Chloro and 4-chlorophenyl analogs (**15m–n**) also demonstrated superior hFAAH and rFAAH potency, and the combination of 3,4-dihalogenation resulted in potent analogs such as **15o–p**.

Truncated aryl tail analogs from the 1-oxa-8-azaspiro[4.5]decane series (**16a–j**) were generally two- to five-fold less potent that the corresponding analogs from the 7-azaspiro[3.5]nonane series (e.g., compare **16a–15a**, **16b–15f**, and **16h–15p**). General SAR trends noted above for the substitution pattern on the aryl group was consistent for both series (e.g., **16a–h**) with small lipophilic groups being preferred substituents in the 3-position. In contrast, small polar groups such as cyano were not tolerated (**16i–j**). As

was observed for lead compound **4**,[3] both enantiomers retained activity similar to the racemate (**16f**).
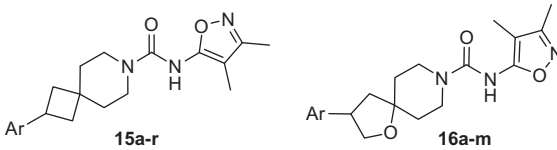
Having established small lipophilic groups as optimal replacements for the biaryl ether in the 7-azaspiro[3.5]nonane series, we turned our focus towards optimization of the heteroaromatic urea leaving group. For this, we selected a few optimal tail groups (e.g., 3-trifluoromethoxyphenyl) and prepared the requisite amine (e.g., **17**; Scheme 3).[6] Amines such as **17** could be converted directly to the desired ureas **18** as described above or first converted to nitrophenyl carbamate **19** which was then reacted with an array of heteroaromatic amines to give a broader collection of ureas **18** after purification by reverse phase HPLC. Targeting access to FAAH in the CNS compartment, we designed libraries of heterocyclic ureas wherein no H-bond donors were added to the final products (i.e., the requisite primary amino heterocycles did not contain additional H-bond donors).

Using this approach, more than 70 ureas were prepared on the 3-trifluormethyoxyphenyl 7-azaspiro[3.5]nonane scaffold. A plot of hFAAH activity as a function of heteroaromatic group reveals a rather remarkable sensitivity to the makeup of the heterocyclic leaving group (Fig. 3). Out of 72 examples, only four examples had FAAH k_{inact}/K_i potency values greater than 2500 M^{-1} s^{-1}. Specific examples are shown in Table 2. The most potent heteroaromatic groups identified were 1-methyltetrazole and 1-ethyltetrazole with roughly five- and two-fold potency enhancements over 3,4-dimethylisoxazol-5-yl (entries 1–2 and 5). Remarkably, the 2-methyltetrazole isomer was ~100-fold less active than the 1-methyl isomer (entry 3) and no FAAH activity was detected for the corresponding methyltriazole derivative (entry 4). A similar level of sensitivity was observed for the isoxazol-5-yl series. The 3-ethyl-4-methylisoxazol-5-yl analog lost only twofold FAAH potency relative to the dimethyl isomer (entries 5 and 6) while 4-ethyl-3-methyl isomer was nearly 10-fold less potent (entry 7). Deletion of the 4-methyl group (entry 8) or reversal of the O and N atoms (entry 9) resulted in more than 20-fold potency reductions. The only other heterocycle identified with retention of FAAH potency was 5-methyl-1,3,4-oxadiazol-2-yl (entry 10).

Given the superior potency observed with 1-methyltetrazole ureas (e.g., **18a**), several of the optimal truncated tail templates (e.g., 3-CF$_3$O, 3-CF$_3$, 3-Cl and 3-Cl,4-F) from both the 7-azaspiro[3.5]nonane and 1-oxa-8-azaspiro[4.5]decane series were combined with 5-amino-1-methyltetrazole using the nitrophenyl carbamate synthetic methodology shown in Scheme 3. Representative compounds obtained are shown in Table 3. Examples from the 7-azaspiro[3.5]nonane series (**18a**, **20–21**) have exceptional potency for hFAAH and sufficient potency for rFAAH. The corresponding 1-oxa-8-azaspiro[4.5]decane analogs (**22–24**) are also quite potent, albeit at a two- to fourfold reduction.

Compounds with suitable FAAH potency (FAAH k_{inact}/K_i >2500 M^{-1} s^{-1}) were resynthesized[6] profiled for selectivity versus the serine hydrolase super family of enzymes (>200 human enzymes, including FAAH), as previously described.[8] The compounds were assayed at 100 μM in a functional proteomic screen based on competitive activity-based protein profiling (ABPP) in human brain membrane and soluble liver proteomes using a rhodamine-tagged fluorophosphonate ABPP probe (ActivX screen). Sufficiently potent compounds that demonstrated selectivity for FAAH in the ActivX, dofetilide and CYP inhibition counter screens were advanced to a screen of oral efficacy in the rat Complete Fruend's Adjuvant (CFA) pain model (Fig. 4 and Table 4).[9,10] This experiment was a key decision making assay which enabled us to determine both pharmacokinetic (PK) parameters and in vivo efficacy; importantly, this assay afforded the ability to move quickly from compound synthesis to selection of preclinical candidates. In practice, compounds were initially screened at an oral fixed dose of 3 mpk. Three h post dose, the FAAH inhibition

Table 1
Representative truncated compounds from tail group optimization

Compd	Ar	hFAAH k_{inact}/K_i[a] (M^{-1} s^{-1})	rFAAH k_{inact}/K_i (M^{-1} s^{-1})[a]	MW	$c \log P$
2b	3-((5-(Trifluoromethyl)pyridin-2-yl)oxy)phenyl	1760	9460	500	4.6
15a	Phenyl	2080	679	339	3.0
15b	2-Methoxyphenyl	2640	265	369	2.5
15c	3-Methoxyphenyl	2190	741	369	2.9
15d	4-Methoxyphenyl	1760	585	369	2.9
15e	2-(Trifluoromethoxy)phenyl	839	564	423	3.6
15f	3-(Trifluoromethoxy)phenyl	2830	3860	423	4.0
15g	4-(Trifluoromethoxy)phenyl	353	229	423	4.0
15h	2-(Trifluoromethyl)phenyl	1140		407	3.9
15i	3-(Trifluoromethyl)phenyl	3060	3690	407	3.9
15j	4-(Trifluoromethyl)phenyl	245	348	407	3.9
15k	3-Methylphenyl	2870	1620	353	3.5
15l	3-Ethylphenyl	5670	1340	367	4.0
15m	3-Chlorophenyl	3940	3560	373	3.7
15n	4-Chlorophenyl	2030	2070	373	3.7
15o	3,4-Dichlorophenyl	4550	3470	407	4.3
15p	3-Chloro-4-fluorophenyl	4190	5820	391	3.8
(±)-**16a**	Phenyl	461	315	355	1.4
(±)-**16b**	3-(Trifluoromethoxy)phenyl	1800	3110	439	2.5
(±)-**16c**	4-(Trifluoromethoxy)phenyl	162	461	439	2.5
(±)-**16d**	3-(Trifluoromethyl)phenyl	1330	2680	423	2.3
(±)-**16e**	4-(Trifluoromethyl)phenyl	481	714	423	2.3
(±)-**16f**	3-Chlorophenyl	2040	2670	389	2.1
16f-ent1	3-Chlorophenyl	2390	1560	389	2.1
16f-ent2	3-Chlorophenyl	2590	3830	389	2.1
(±)-**16g**	3,4-Dichlorophenyl	2430	4360	423	2.7
(±)-**16h**	3-Chloro-4-fluorophenyl	1580	3950	407	2.3
(±)-**16i**	3-Cyanophenyl	243	999	380	0.9
(±)-**16j**	4-Cyanophenyl	43.2	26.1	380	0.9

[a] Each k_{inact}/K_i value corresponds to an average of at least two independent determinations.
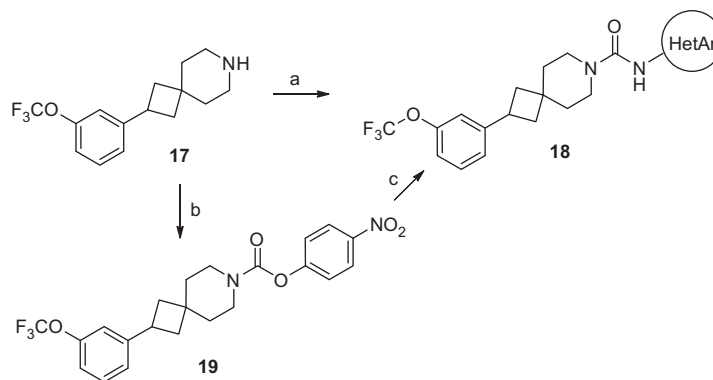
Scheme 3. Preparation of urea libraries. Reagents and conditions:[6] (a) **10**, DIEA, CH$_3$CN, room temp; (b) 4-nitrophenyl chloroformate, dioxane, satd sodium bicarbonate (92%); (c) H$_2$N-HetAr, NaH, DMA.

in the brain as well as compound concentration in the brain and plasma were determined. Additionally, to facilitate estimation of rat clearance values, compound plasma concentrations at 24 h were determined.

With the ultimate goal of choosing the 'best' compound suitable for QD dosing with good safety margins, a few key factors were emphasized during the screening process. First, it was necessary to have sufficient brain exposure relative to potency to achieve >95% FAAH inhibition; this defined the minimum efficacious dose

(MED). It was also desirable for a compound to have a low efficacious concentration ($C_{eff} \sim C_{min}$), resulting a low dose, and a shallow C_{max}/C_{min} profile in plasma. In general, rat clearance values of <15 mL/min/kg, coupled with FAAH potency k_{inact}/K_i >2500 M^{-1} s^{-1}, was optimal for a low dose QD profile. More detailed evaluation of the dose response relationships for several compounds in the CFA model, enabled us to develop the correlation between in vitro potency, exposure and MED.[11,12] As shown in Figure 4, it was determined that, in general, a [brain]/K_i >0.2
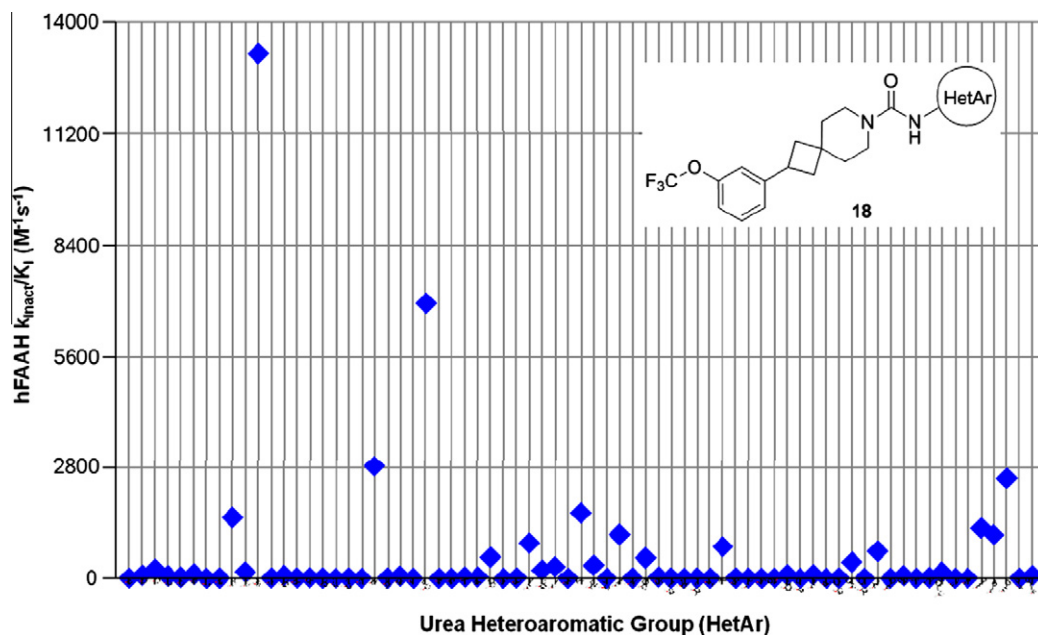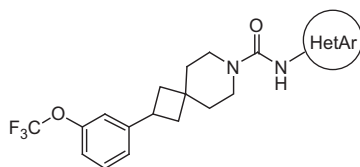
Figure 3. Urea group SAR.

Table 2
Urea heteroaromatic group SAR

Entry	Compd	HetAr	hFAAH k_{inact}/K_i[a] (M^{-1} s^{-1})	rFAAH k_{inact}/K_i[a] (M^{-1} s^{-1})	MW	$c \log P$
1	**18a**		13,200	4570	410	3.7
2	**18b**		6940	3420	424	4.2
3	**18c**		165	152	410	2.6
4	**18d**		<10	—	409	3.3
5	**15f**		2830	3860	423	4.0
6	**18e**		1650	1660	437	4.5
7	**18f**		338	—	437	4.5
8	**18g**		113	—	409	4.4
9	**18h**		64	34.2	423	4.0

Table 2 (continued)

Entry	Compd	HetAr	hFAAH k_{inact}/K_i[a] (M^{-1} s^{-1})	rFAAH k_{inact}/K_i[a] (M^{-1} s^{-1})	MW	$c \log P$
10	**18i**		1530	2460	410	3.3

[a] Each k_{inact}/K_i value corresponds to an average of at least two independent determinations.

Table 3
1-Methyltetrazole tail group SAR
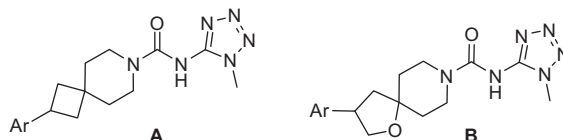
| Compd	Ar	Series	hFAAH k_{inact}/K_i[a] (M^{-1} s^{-1})	rFAAH k_{inact}/K_i[a] (M^{-1} s^{-1})	MW	$c \log P$
18a	3-(Trifluoromethoxy)phenyl	A	13,200	4570	410	3.7
20	3-(Trifluoromethyl)phenyl	A	12,400	5750	394	3.5
21	3-Chloro-4-fluorophenyl	A	16,300	5940	379	3.5
22-ent1	3-(Trifluoromethoxy)phenyl	B	7110	4560	426	2.1
23-ent1	3-(Trifluoromethyl)phenyl	B	4600	2160	410	2.0
23-ent2	3-(Trifluoromethyl)phenyl	B	3760	2110	410	2.0
24-ent1	3-Chlorophenyl	B	5600	1970	377	1.8

[a] Each k_{inact}/K_i value corresponds to an average of at least two independent determinations.

was required for efficacy. Importantly, this single experiment provided information on target inhibition at the site of action ([brain]/K_i), PK profile and their relationship to efficacy.

For further prioritization purposes, human PK parameters were estimated from this single point efficacy/PK experiment utilizing allometric scaling from the estimated rat PK.[13] Rat clearance was estimated from the 3 h and 24 h time points. We assumed that both the absorption constant (K_a) and volume of distribution were relatively invariant across similar chemical space. We took a conservative approach to human dose setting and assumed that efficacy required 24 h coverage of the C_{eff} derived from the CFA studies (i.e., $C_{min} > C_{eff}$). This exposure was likely higher than that required at 24 h to maintain efficacy. The predicted human dose and pharmacokinetic profile, including the estimated C_{max} and C_{max}/C_{min} ratio, proved to be useful tools for prioritization of compounds before

advancement to more resource and time intensive studies. The most promising compounds were selected for a more complete analysis including a dose-response study in the CFA model and IV/PO rat PK. This enabled a more definitive projection of human PK and C_{eff} using multiple data points and the generation of an EC_{95} based upon a simple E_{max} model relating %FAAH inhibition in the brain to compound plasma exposure. Importantly, for the compounds which we conducted this more rigorous analysis, there was good agreement with the data estimated from the screening model (Table 4).

On the basis of the in vivo efficacy/PK screen and subsequent dose response efficacy experiments, compound **15p** was selected as a candidate for human clinical trials. This compound has calculated properties consistent with that for known CNS drugs (MW = 391, $c \log P$ = 3.8, tPSA = 58 Å^3) and clean selectivity profiles in CYP, hERG, Ames, micronucleous, and CEREP assays (data not shown). Furthermore, characterization in the ActivX selectivity screen, **15p** was found to inhibit only FAAH at concentrations up to 100 μM. In rats, **15p** has a half-life of 7.1 h (CL = 8.5 mL/min/
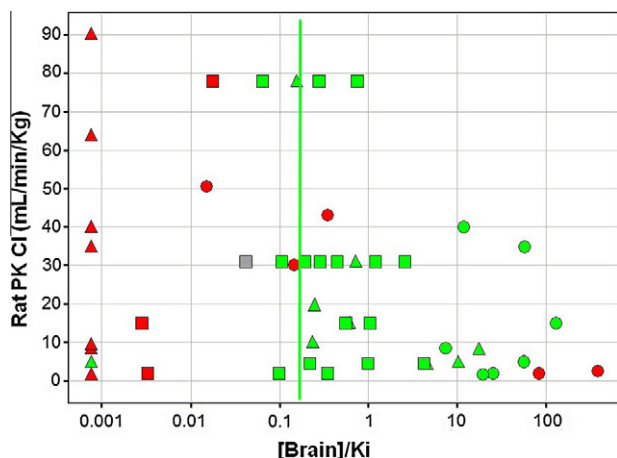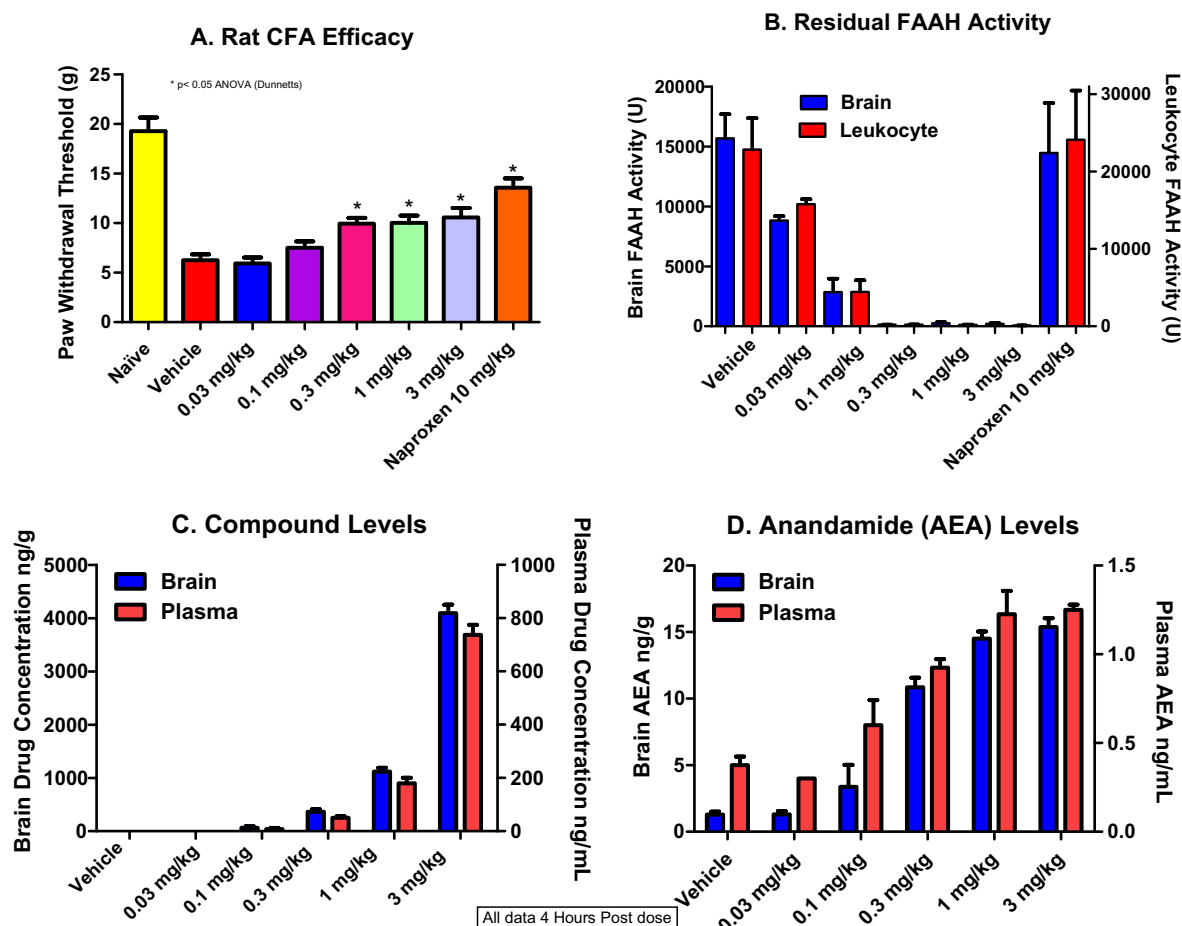
Figure 4. The correlation between efficacy and brain/K_i across several compound classes.[3,4] Colored by efficacy in the CFA assay: green = active, red = inactive; and shaped by dose: ▲ = single dose PO, ● = single dose IP, ■ = dose response PO. Single point studies were 3 mpk, 10 mpk or 25 mpk.

Table 4
In vivo efficacy data for representative compounds

Compd	hFAAH k_{inact}/K_i[a] (M^{-1} s^{-1})	rFAAH k_{inact}/K_i[a] (M^{-1} s^{-1})	CFA 3 mpk PO	Predicted CFA MED (mpk)	Actual CFA MED (mpk)
15f	2830	3860	Active	0.5	1
15l	5670	1340	Inactive	N/A	N/A
15m	3940	3560	Active	0.8	1
15p	4190	5820	Active	0.1	0.3
18a	13,200	4570	Active	0.04	0.1
20	12,400	5750	Active	0.2	1
22-ent1	7110	4560	Active	0.1	0.3
23-ent1	4600	2160	Active	1.0	0.1

[a] Each k_{inact}/K_i value corresponds to an average of at least two independent determinations.

6552

M. J. Meyers et al./Bioorg. Med. Chem. Lett. 21 (2011) 6545–6553

Figure 5. Effect of compound **15p** in the CFA model of inflammatory pain: relationship between efficacy, PK, and modulation of target and mechanism biomarkers. All samples were taken 4 h post dose. All PK/biomarker samples and behavioural assessments were taken from the same animals. (A) Paw withdrawal threshold assessment via von Frey filaments. $N = 8$ animals/group. *Significance with respect to vehicle ($p < 0.05$, ANOVA/Dunnetts). (B) Residual FAAH activity from brain tissue or leukocytes were measured in a FAAH assay with ^{3}H-anandamide as substrate. (C and D) Compound and AEA levels were determined by LC/MS. (B, C and D) $n = 4$ animals/group.

kg, $V_{dss} = 3.4$ L/kg) and 53% bioavailability. Similarly, in dogs, **15p** has a half-life of 7.8 h (CL = 11.1 mL/min/kg, $V_{dss} = 5.0$ L/kg) and 33% bioavailability. In the rat CFA model, **15p** has a MED of 0.3 mpk (Fig. 5A). At 0.3 mpk, residual FAAH activity is completely inhibited in both leukocytes and brain isolates, corresponding to 0.459 μM plasma concentration of **15p** (Fig. 5B and C). As expected, levels of the FAAH substrate AEA were elevated in a dose-dependent manner (Fig. 5D), consistent with the observed efficacy and residual FAAH activity data.

In summary, we have optimized the spirocyclic 7-azaspiro[3.5]nonane and 1-oxa-8-azaspiro[4.5]decane cores for FAAH potency, identifying leads with significantly reduced molecular weights and favorable CNS drug-like properties. Additionally, 3,4-dimethylisoxazole and 1-methyltetrazole were identified as superior urea moieties for inhibition of FAAH. Once suitable low molecular weight tail groups and urea heterocycles were identified, the most promising compounds were advanced using the ActivX selectivity panel and CFA efficacy assay to select preclinical candidates. On the basis of the remarkable potency, selectivity, pharmacokinetic properties and in vivo efficacy, **15p** was advanced as a clinical candidate.

Acknowledgments

References and notes

1. Ahn, K.; McKinney, M. K.; Cravatt, B. F. *Chem. Rev.* **2008**, *108*, 1687.
2. (a) Lambert, D. M.; Fowler, C. J. *J. Med. Chem.* **2005**, *48*, 5059; (b) Pacher, P.; Batkai, S.; Kunos, G. *Pharmacol. Rev.* **2006**, *58*, 389; (c) Di Marzo, V. *Nat. Rev. Drug Disc.* **2008**, *7*, 438.
3. Meyers, M. J.; Long, S. A.; Pelc, M. J.; Wang, J. L.; Bowen, S. J.; Walker, M. C.; Schweitzer, B. A.; Madsen, H. M.; Tenbrink, R. E.; McDonald, J.; Smith, S. E.; Foltin, S.; Beidler, D.; Thorarensen, A. *Bioorg. Med. Chem. Lett.* The previous manuscript in this issue.
4. Johnson, D. S.; Stiff, C.; Lazerwith, S. E.; Kesten, S. R.; Fay, L. K.; Morris, M.; Beidler, D.; Liimatta, M. B.; Smith, S. E.; Dudley, D. T.; Sadagopan, N.; Bhattachar, S. N.; Kesten, S. J.; Nomanbhoy, T. K.; Cravatt, B. F.; Ahn, K. *ACS Med. Chem. Lett.* **2011**, *2*, 91.
5. Hitchcock, S. A.; Pennington, L. D. *J. Med. Chem.* **2006**, *49*, 7559.
6. (a) For detailed experimental procedures for the preparation of 7-azaspiro[3.5]nonane series 1-oxa-8-azaspiro[4.5]decane compounds, see: Meyers, M. J.; Schweitzer, B. A.; Pelc, M.; Wang, J. L.; Long, S. A.; Thorarensen, A. WO2010/049841, 2010.; (b) For detailed experimental procedures for the preparation of 1-oxa-8-azaspiro[4.5]decane compounds, see: Long, S. A.; Wang, J. L.; Meyers, M. J.; Pelc, M.; Schweitzer, B. A.; Thorarensen, A. WO2010/058318, 2010.
7. (a) Gonzalez-Bobes, F.; Fu, G. C. *J. Am. Chem. Soc.* **2006**, *128*, 5360; (b) *Note:* This chemistry only worked on small scale; when a larger quantity of a specific compound was desired, a sequence similar to Scheme 1 was utilized.
8. (a) Cravatt, B. F.; Wright, A. T.; Kozarich, J. W. *Annu. Rev. Biochem.* **2008**, *77*, 383; (b) Liu, Y.; Patricelli, M. P.; Cravatt, B. F. *Proc. Natl. Acad. Sci. U.S.A.* **1999**, *96*,

14694; (c) Ahn, K.; Johnson, D. S.; Fitzgerald, L. R.; Liimatta, M.; Arendse, A.; Stevenson, T.; Lund, E. T.; Nugent, R. A.; Nomanbhoy, T. K.; Alexander, J. P.; Cravatt, B. F. *Biochemistry* **2007**, *46*, 13019.
9. Ahn, K.; Johnson, D. S.; Mileni, M.; Beidler, D.; Long, J. Z.; McKinney, M. K.; Weerpana, E.; Sadagopan, N.; Liimatta, M.; Smith, S. E.; Lazerwith, S.; Stiff, C.; Kamtekar, S.; Bhattacharya, K.; Zhang, Y.; Swaney, S.; Becelaere, K. V.; Stevens, R. C.; Cravatt, B. F. *Chem. Biol.* **2009**, *16*, 411.
10. The Pfizer Institutional Animal Care and Use Committee reviewed and approved the animal use in these studies. The animal care and use program is fully accredited by the Association for Assessment and Accreditation of Laboratory Animal Care, International.
11. Calculation of [brain]/K_i was estimated by: $[brain] * (k_{inact}/K_i)/k_{inact}$. This required the assumption that the k_{inact} was constant and we utilized a value for $k_{inact} = 0.00265\ s^{-1}$. The MED and subsequently the [plasma] exposure at

the MED was then predicted using the above knowledge. A linear dose relationship was assumed for all compounds allowing calculation of these values. MED dose calculation is the simplified equation: (CFA-SP dose/([brain]$_{SP}$/K_i)) = (MED dose/0.2). Example calculation for **15p**: rFAAH = 4900 $M^{-1}\ s^{-1}$; [brain]$_{SP}$ = 2.44 μM; [brain]/K_i = 4.52; CFA-SP dose = 3 mpk; MED-pred = 3 mpk/4.52 * 0.2 = 0.12 mpk; actual MED = 0.3 mpk]. Plasma exposure at MED: [plasma]$_{MED}$ = ([plasma]$_{SP}$/CFA-SP dose) * MED dose pred.

12. Maurer, T. S.; DeBartolo, D. B.; Tess, D. A.; Scott, D. O. *Drug Metab. Dispos.* **2005**, *33*, 175.
13. Hosea, N. A.; Collard, W. T.; Cole, S.; Maurer, T. S.; Fang, R. X.; Jones, H.; Kakar, S. M.; Nakai, Y.; Smith, B. J.; Webster, R.; Beaumont, K. *J. Clin. Pharmacol.* **2009**, *49*, 513.